





In this paper, to establish the theoretical model for studying the mass weighing approach at a fixed exciting frequency, a mechanical-electrical coupling model is established for calculating the impedance variation induced by mass-change. Through the impedance analysis of the simplified mass weighing approach, the complex relationship among the exciting frequency, geometrical parameters, and dynamic response has been theoretically analyzed, with which, the system parameters such as the fixed exciting frequency and the linear impedance-frequency range can be properly adjusted or designed for different applications. And, with the proposed model, the strategy for selecting the fixed exciting frequency in the vicinity of resonant frequency to achieve maximum sensitivity obtained from Xu and Raj Mutharasan's experiments is theoretically validated. A macro-sized cantilever sensor of 26.0 mm long is fabricated, whose second order resonant frequency is 3114.9Hz about 4.22% deviated from the theoretical value of 3252.0Hz. By exciting the cantilever at the resonance frequency, the measured impedance and sensitivity are  $2.49 \times 10^4 \Omega$  and 514.8 $\Omega$ /mg which are only about 1.92% and 4.4% deviated from the theoretical  $2.444 \times 10^4 \Omega$  and 537.5 $\Omega$ /mg. More importantly, the obtained impedance sensitivity is almost 58.4 times greater than the resonant frequency based sensitivity of 9.2Hz/mg. Considering the manufacturing errors, the theoretical results are nearly consistent with those by experiments, thus, the effectiveness of the proposed equivalent circuit model is adequately verified, which is really crucial and useful for simplifying the mass weighing procedure and improving sensor performances to desired degree for different applications.

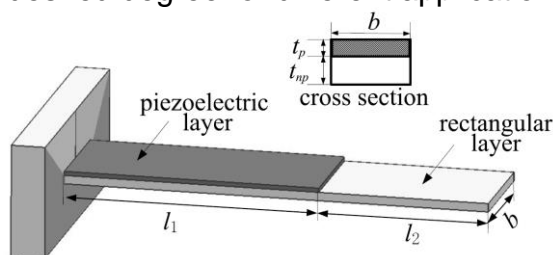


Figure 1 | Structure of piezoelectric cantilever mass sensor

## 2. Mechanical-electrical coupling model of the cantilever mass sensor

Ordinarily, a piezoelectric layer bonded with an elastic rectangular layer as shown in Fig.1 acts both as a actuating and sensing element in the cantilever mass sensor. When the AC voltage  $V(t) = V_0 e^{j\omega t}$  is applied on the top and bottom surfaces, the piezoelectric layer will cause the sensor in bending vibration. And meanwhile, the mass change will directly induce changes of the dynamic resonance. In Fig.1,  $l_1$  and  $l_2$  are the length of the piezoelectric layer and the extension respectively,  $b$  is the width of the rectangular beam,  $t_p$  and  $t_{rp}$  are the thickness of the piezoelectric layer and the elastic cantilever.

The equation of motion for the lateral vibration of the piezoelectric actuated composite cantilever, including the effect of damping, can be written as

$$m(x) \frac{\partial^2 w(x,t)}{\partial t^2} + c_p \frac{\partial w(x,t)}{\partial t} + \frac{\partial^2}{\partial x^2} \left( EI(x) \frac{\partial^2 w(x,t)}{\partial x^2} \right) = M(t) \quad (1)$$

where  $w(x,t)$  is the transverse displacement,  $f(x,t)$  is the applied driving force with frequency  $\omega$ ,  $m(x)$  is the mass of unit length,  $E$  is the elastic modulus,  $I(x)$  is the moment of inertia,  $c_p$  is the damping coefficient.

From the piezoelectric actuation principle, the generated equivalent moment  $M$  acting on the free end of the piezoelectric layer can be obtained. By setting the free end of the piezoelectric layer as the coordinate origin, the equivalent moment  $M(t)$  at the origin can be expressed as follows.

$$M(t) = \frac{bd_{31}E_{np}t_{np}(t_p + t_{np})^2}{2s_{11}^E t_p (E_{np}t_{np} + E_p t_p)(E_p t_p + E_p t_{np})} V_0 e^{j\omega t} \quad (2)$$

Where  $b$  is the width of the piezoelectric layer,  $d_{31}$  is the piezoelectric strain coefficient,  $E_p$ ,  $E_{np}$ ,  $t_p$  and  $t_{np}$  are the elastic modulus and thickness of the piezoelectric layer and elastic layer,  $s_{11}^E$  is the elastic compliance coefficient under constant electric field,  $V_0$  the applied voltage amplitude.

By applying orthogonal conditions of the normal modes, the uncoupled ordinary differential equations for the generalized coordinates,  $q_n(t)$  can be obtained as

$$\ddot{q}_n(t) + 2\xi_n \omega_n \dot{q}_n(t) + \omega_n^2 q_n(t) = Q_n(t) \quad (3)$$

Where  $\xi_n$  is the damping ratio of  $n$ -order mode,  $\omega_n$  is the  $n^{\text{th}}$  order natural frequency,  $M(t)$  is the generalized moment.

Then, according to the piezoelectric constitutive equations, the unit surface charge  $D_3$  of the piezoelectric layer can be determined according to the inverse piezoelectric effects.

$$Q = b \int_{-l_1}^0 \left( \left( \epsilon_{33}^T - \frac{d_{31}^2}{s_{11}^E} \right) E_3 + \frac{d_{31}}{s_{11}^E} S_1 \right) dx \quad (2)$$

Where  $S_1$  is the surface strain,  $s_{11}^E$  is the elastic compliance coefficient under constant electric field,  $\epsilon_{33}^T$  is the dielectric constant under constant stress,  $d_{31}$  is the piezoelectric strain coefficient, and  $E_3$  is the electric field intensity.

### Equivalent impedance analyzing for the piezoelectric cantilever mass sensor

According to the BVD equivalent circuit model [18] shown in figure 2, the piezoelectric layer operating at resonance frequency can be simplified as two parallel branches that static capacitance  $C_0$  and dynamic parameters including dynamic capacitance ( $C_m$ ), dynamic inductor ( $L_m$ ) and dynamic resistance ( $R_m$ ) respectively. Except for the static capacitance, the dynamic parameters are heavily related to the response of the composite

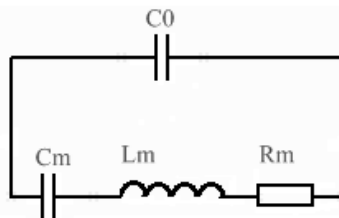


Figure 2 BVD equivalent circuit model from reference [18]

cantilever obtained from the mechanical-electrical coupling analysis.

The static capacitance  $C_0$  can be defined according to the capacitance's constitutive equation.

$$C_0 = \frac{l_1 b}{t_p} \left( \varepsilon_{33}^T - \frac{d_{31}^2}{s_{11}^E} \right) \quad (3)$$

According to the circuit theory, the dynamic admittance reaches the maximum value at the resonant frequency,  $\omega = \omega_n$ .

$$G_{\max} = j \frac{E_{np} t_{np} t_n \varphi_{n1}'(0) H(\omega) (t_p + t_{np})^2}{2 t_p m_n^e \omega_n (E_{np} t_{np} + E_p t_p) (E_p t_p + E_p t_{np})} \left( \frac{b d_{31}}{s_{11}^E} \right)^2 \int_{-l_1}^0 \frac{\partial^2 \varphi_{n1}(x)}{\partial x^2} dx \quad (4)$$

Also known, the quality factor  $Q_{nm}$  can be determined.

$$\begin{cases} H(\omega_n) = -jQ_{nm} \\ Q_{nm} = \frac{1}{2\xi_n} \\ Q_{nm} = \frac{1}{R_m} \sqrt{L_m / C_m} \\ \omega_n L_m = 1 / (\omega_n C_m) \end{cases} \quad (5)$$

With the dynamic admittance in equation (29), the dynamic capacitance and inductance can be expressed by the known parameters of resonance frequency and quality factor in equation (30).

$$\begin{cases} C_m = \frac{1}{\omega_n R_m Q_{nm}} \\ L_m = \frac{R_m Q_{nm}}{\omega_n} \end{cases} \quad (6)$$

Then, the Parallel circuit impedance can be determined.

$$Z = R_e + jX_e \quad (7)$$

in which the resistance component and reactance component are

$$\begin{cases} R_e = \frac{R_m / (\omega^2 C_0^2)}{R_m^2 + \left( \omega L_m - \frac{1}{\omega C_m} - \frac{1}{\omega C_0} \right)^2} \\ X_e = \frac{\frac{1}{\omega C_0} \left[ R_m^2 + \left( \omega L_m - \frac{1}{\omega C_m} \right) \left( \omega L_m - \frac{1}{\omega C_m} - \frac{1}{\omega C_0} \right) \right]}{R_m^2 + \left( \omega L_m - \frac{1}{\omega C_m} - \frac{1}{\omega C_0} \right)^2} \end{cases} \quad (8)$$

Then, the impedance variation  $\Delta Z$  induced by the added mass can be determined.

$$\Delta Z = \sqrt{\frac{R_m^2}{\alpha} + \frac{\left( R_m^2 + \left( \omega_n L_m - \frac{1}{\omega_n C_m} \right) \left( \omega_n L_m - \frac{1}{\omega_n C_0} - \frac{1}{\omega_n C_m} \right) \right)^2}{\alpha}} + \sqrt{\frac{\left( R_m^2 + \left( \omega_n L_m - \frac{1}{\omega_n C_m} \right) \left( \omega_n L_m - \frac{1}{\omega_n C_0} - \frac{1}{\omega_n C_m} \right) \right)^2}{(\omega_n C_0 \beta)} + \frac{R_m^2}{\omega_n^4 C_0^4 \beta}} \quad (9)$$

Where

$$\alpha = \omega_n^4 C_0^2 \left( R_m^2 + \left( \omega_n L_m - \frac{1}{\omega_n C_0} - \frac{1}{\omega_n C_m} \right)^2 \right)^2 \quad (10)$$

$$\beta = \left( R_m^2 + \left( \omega_n L_m - \frac{1}{\omega_n C_m} - \frac{1}{\omega_n C_0} \right)^2 \right)^2 \quad (11)$$

## Experiments

The structure parameters of the piezoelectric cantilever micro-mass sensor are listed in Table 1. The impedance curves are plotted for the cantilever sensor operating in the second-order mode, as shown in Fig.3.

Tab. 1 Basic dimensions of the mass sensor

Parameters	Rectangular layer	Piezoelectric layer
length/mm	26.0	8.0
width/mm	4.0	4.0
thickness/mm	0.4	0.2
elasticity modulus/GPa	196.5	76.5
density/kg/m <sup>3</sup>	7.8×10 <sup>3</sup>	7.5×10 <sup>3</sup>

From figure 3, it can be seen that the second-order mode resonant frequency of the cantilever sensor is 3252.0Hz. And the impedance varies linearly with the exciting frequency in the frequency range from 3206.0 Hz to 3305.0 Hz. So, any frequency in this range can be chosen as the detection frequency for the mass sensing application. For example, at the resonant frequency, curve 'a' and curve 'b' represent the impedances of two cases that loading mass and not loading mass. Then, the impedance variation between the two curves at frequency 3252.0Hz can be used to determine the weight of the added mass.

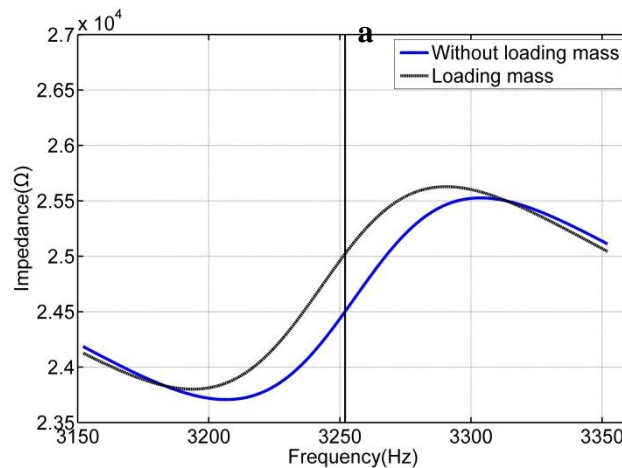
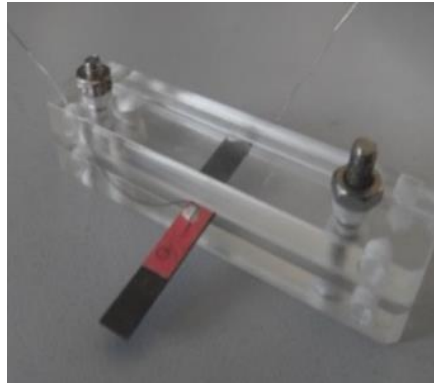


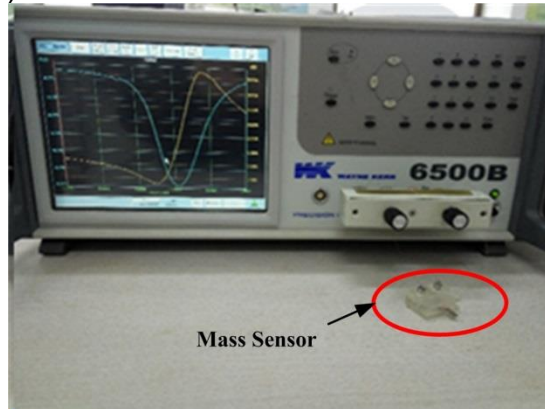
Figure 3| Curve of impedance versus frequency in the vicinity of the second-order mode

In order to validate the effectiveness of the proposed model, a macro-sized cantilever sensor of 4.0mm wide and 26.0mm long is fabricated, whose theoretical second order resonant frequency is 3252.0Hz about 4.22% deviated from the

measured value of 3114.9Hz, as shown in figure 4, the sensitivity was measured using a precision impedance analyzer (WK6500B). Due to the impact of conductive adhesive coating and the quality of the connecting wire, the experimental obtained resonant frequency is lower compared to the theoretical results, and thus, resulting in higher impedance.

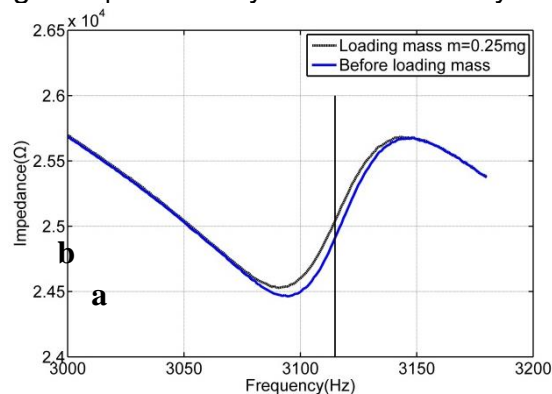


(a) Piezoelectric cantilever micro-mass sensor

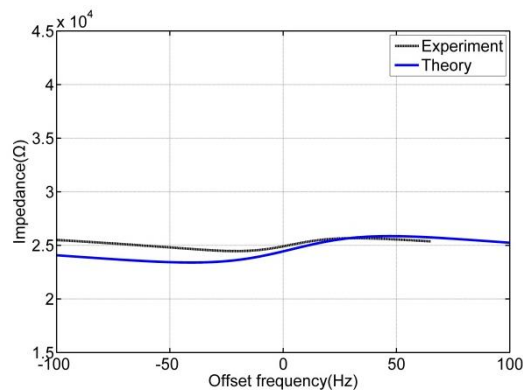


(b) Sensor test system

Figure 5| Sensitivity measurement system



(a) The experimental impedance curve



(b) Impedance curve comparison

Fig.6 Comparison of experimental and theoretical curves

By selecting the resonance frequency of 3114.9 Hz as the fixed exciting frequency, the measured impedance and the sensitivity are  $2.49 \times 10^4 \Omega$  and  $514.8 \Omega/\text{mg}$ , which are about 1.92% and 4.4% deviated from the theoretical values of  $2.444 \times 10^4 \Omega$  and  $537.5 \Omega/\text{mg}$ . Considering influences of the manufacturing and fabricating errors, the deviation between the theoretical and experimental results is in an acceptable level.

Also, the whole linear frequency bandwidth is 22.0 Hz. And the theoretical maximum impedance is  $2.586 \times 10^4 \Omega$  about 0.7% deviated from the experimental result of  $2.568 \times 10^4 \Omega$ . Meanwhile, the minimum impedance is  $2.342 \times 10^4 \Omega$  about 4.52% deviated from the experimental value of  $2.448 \times 10^4 \Omega$ . Then, it can be concluded that the proposed theoretical model can precisely predict the detecting frequency range for the cantilever mass sensor.

In the vicinity of the resonant frequency, the bandwidth of the impedance based mass measurement is very narrow, which directly leads to the limitation on the maximum detectable weight of 2.5 mg. Generally without the procedure of wide range frequency sweeping, the mass measurement can be quickly completed with a high impedance sensitivity which is almost 58.4 times greater than that from the frequency based method. Hence, such fixed frequency impedance monitoring approach can not only breakthrough limitation of the frequency-sweep method requiring complex measuring instruments, but also can significantly increase the sensitivity and reduce the detecting time, which is really crucial for promoting piezoelectric mass sensors to be applicable in hash detection environments.

## Conclusion

A mechanical-electrical model based on the equivalent circuit model is established for calculating the impedance based sensitivity of the resonant mass sensor operating at a fixed frequency. And the complex coupling effects among the dynamic response, structure parameters, excitation frequency and equivalent impedance has been revealed, which is crucial for determining key system parameters e.g. the fixed exciting frequency, the linear impedance-frequency range and piezoelectric parameters. It can also be concluded that the sensitivity varies with the exciting frequency and the optimum exciting point locates at the frequency close to the resonant frequency, which is consistent with the that from Xu and Raj Mutharasan. A macro-sized cantilever sensor of 26.0 mm long is fabricated, whose second order resonant frequency is



3114.9Hz about 4.22% deviated from the theoretical value of 3252.0Hz. By exciting the cantilever at the resonance frequency, the measured impedance and sensitivity are  $2.49 \times 10^4 \Omega$  and 514.8 $\Omega$ /mg which are only about 1.92% and 4.4% deviated from the theoretical  $2.444 \times 10^4 \Omega$  and 537.5 $\Omega$ /mg. More importantly, the obtained impedance sensitivity is almost 58.4 times greater than the resonant frequency based sensitivity of 9.2HZ/mg. Generally speaking, without the procedure of wide range frequency sweeping, the mass measurement can be quickly completed with a high sensitivity which is almost 58.4 times greater than that from the frequency based method. Considering the manufacturing errors, the theoretical results are nearly consistent with those by experiments, thus, the effectiveness of the proposed equivalent circuit model is adequately verified.

## References

1. Fritz, J., Baller, M.K., Lang, H.P., Rothuizen, H., Vettiger, P., Meyer, E., Guntherodt, H.-J., Gerber, C., Gimzewski, J.K., 2000. Translating biomolecular recognition into nanomechanics. *Science* 288 (5464), 316–318.
2. Lee J. H., Kim T. S., Yoon K. H., 2004. Effect of mass and stress on resonant frequency shift of functionalized Pb(Zr<sub>0.52</sub>Ti<sub>0.48</sub>)O<sub>3</sub> thin film microcantilever for the detection of C-reactive protein. *Appl. Phys. Lett.*, 84(16), 3187-3189.
3. Boudjiet M T, Bertrand J, Pellet C, et al. New characterization methods for monitoring small resonant frequency variation: Experimental tests in the case of hydrogen detection with uncoated silicon microcantilever-based sensors[J]. *Sensors & Actuators B Chemical*, 2014, 199(6):269-276.
4. Mcgrath T F, Elliott C T, Fodey T L. Biosensors for the analysis of microbiological and chemical contaminants in food.[J]. *Analytical & Bioanalytical Chemistry*, 2012, 403(1):75.
5. Wu G. H., Datar R. H., Hansen K. M., Thundat T., Cote R. J., and Majumdar A., 2001. Bioassays of prostate-specific antigen (PSA) using microcantilevers. *Nature Biotechnol.*, 19, 856–860.
6. Sharma H, Mutharasan R. Rapid and sensitive immunodetection of *Listeria monocytogenes* in milk using a novel piezoelectric cantilever sensor.[J]. *Biosensors & Bioelectronics*, 2013, 45(2):158-162.
7. Gfeller K. Y., Nugaeva N., and Hegner M., “Micromechanical oscillators as rapid biosensor for the detection of active growth of *Escherichia coli*,” *Biosen. Bioelectron.*, vol. 21, no. 3, pp. 528–533, Dec. 2005.
8. Wasisto H. S., Merzsch S., Waag A., Uhde E., Salthammer T., and Peiner E., “Airborne engineered nanoparticle mass sensor based on a silicon resonant cantilever,” *Sens. Actuators B: Chem.*, vol.180, pp.77-89, Apr. 2013.
9. Zhang H. and Kim E. S., “Micromachined Acoustic Resonant Mass Sensor,” *J. Microelectromechanical Sys.*, vol. 14, no. 4, pp. 699-706, Aug. 2005.
10. Zhou J, Huang L, Fu Z, et al. Multiplexed Simultaneous High Sensitivity Sensors with High-Order Mode Based on the Integration of Photonic Crystal 1 × 3 Beam Splitter and Three Different Single-Slot PCNCs[J]. *Sensors*, 2016, 16(7):1050.
11. Ghatkesar M. K., Barwich V., Braun T., Ramseyer J-P., Gerber Ch., Hegner M., Lang P. L., Drechsler U., and Despont M., “Higher modes of vibration increase

- mass sensitivity in nanomechanical microcantilevers,” *Nanotechnology*, vol. 18, no. 44, pp. 445502(8pp), Nov. 2007.
12. Ghatkesar M. K., Braun T., Barwich V., Ramseyer J-P., Gerber Ch., Hegner M., and Lang P. L., “Resonating modes of vibrating microcantilevers in liquid,” *Appl. Phys. Lett.*, vol. 92, no. 4, pp. 043106, Jan.2008.
  13. Ansari M. Z. and Cho C., “Deflection, Frequency, and Stress Characteristics of Rectangular, Triangular, and Step Profile Microcantilevers for Biosensors,” *Sensors*, vol. 9, no.8, pp. 6046-6057, Jul. 2009.
  14. Thein C K, Liu J S. Numerical modeling of shape and topology optimisation of a piezoelectric cantilever beam in an energy-harvesting sensor[J]. *Engineering with Computers*, 2016:1-12.
  15. Zhao J., Zhang Y., Gao R., Liu S., A new sensitivity improving approach for mass sensors through integrated optimization of both cantilever surface profile and cross-section. *Sensors and Actuators B: Chemical*. 2015, 206:343-350.
  16. Xu S. and Mutharasa Raj., A novel method for monitoring mass-change response of piezoelectric-excited millimeter-sized cantilever (PEMC) sensors. *Sensors & Actuators B Chemical*, 2009, 143(1):144-151.
  17. Ramji S. Lakshmanan, Xu S., Mutharasan Raj. Impedance change as an alternate measure of resonant frequency shift of piezoelectric-excited millimeter-sized cantilever (PEMC) sensors. *Sensors & Actuators B Chemical*. 2010, 145(1): 601-604.
  18. VAN DYKE K. S., Thepiezo-electric resonator and its equivalent network. *Proceedings of the Institute of Radio Engineers*. 1928, 16(6):742-764.